



Contents lists available at ScienceDirect

Bioorganic & Medicinal Chemistry

journal homepage: www.elsevier.com/locate/bmc

Synthesis, structure-activity relationships and preliminary mechanism study of *N*-benzylideneaniline derivatives as potential TLR2 inhibitors

Shaoyi Cai^{a,c}, Gengzheng Zhu^{a,c}, Xiaohong Cen^{a,c}, Jingjie Bi^a, Jingru Zhang^a, Xiaoshan Tang^a, Kun Chen^{b,*}, Kui Cheng^{a,*}

^a Guangdong Provincial Key Laboratory of New Drug Screening and Guangzhou Key Laboratory of Drug Research for Emerging Virus Prevention and Treatment, School of Pharmaceutical Sciences, Southern Medical University, Guangzhou 510515, China

^b The Joint Research Center of Guangzhou University and Keele University for Gene Interference and Application, School of Life Science, Guangzhou University, Guangzhou 510006, China

ARTICLE INFO

Article history:

Received 2 January 2018
Revised 28 February 2018
Accepted 1 March 2018
Available online xxx

Keywords:

Toll-like receptor 2
Small molecule antagonist
Schiff base derivatives
Inflammatory cytokines

ABSTRACT

Toll-like receptor 2 (TLR2) can recognize pathogen-associated molecular patterns to defense against invading organisms and has been represents an attractive therapeutic target. Until today, none TLR2 small molecule antagonist have been developed in clinical trial. Herein, we designed and synthesized 50 *N*-benzylideneaniline compounds with the help of CADD. And subsequent *in vitro* studies leading to the optimized compound SMU-A0B13 with most potent inhibitory activity to TLR2 ($IC_{50}=18.21 \pm 0.87 \mu M$). Preliminary mechanism studies indicated that this TLR2 inhibitor can work through the NF- κB signaling pathway with high specificity and low toxicity, and can also efficiently downregulate inflammatory cytokines, such as SEAP, TNF- α and NO in HEK-Blue hTLR2, human PBMC and Raw 264.7 cell lines. Additionally, the docking situation also indicate SMU-A0B13 can well bind to the TLR2-TIR (PDB: 1FYW) active domain, which probably explains the bioactivity.

© 2018 Elsevier Ltd. All rights reserved.

1. Introduction

Toll-like receptors (TLRs), an essential pattern recognition receptors, are widely expressed in various immune cells of multifarious tissues and organs, regulating innate and acquired immunity response through myeloid differentiation primary response 88 (MyD88) dependent pathway or MyD88 independent pathway^{1,2} by up-regulating the production of cytokines and costimulatory molecules on the antigen-presenting cell (APC) to ensure the organism releases and maintains a suitable level of proinflammatory cytokine.^{3–5} Studies have found that TLRs play an important role in the development of autoimmune diseases, tumors and other intractable disorders.^{6–13} The activation of TLRs leads a train of signal transduction to defense pathogen.¹⁴ However, over-express of TLR will induce too much cytokines leading to inflammation.¹⁵ So the activation of TLR is a double-edged sword and both positive and negative regulation can be used as a target for clinical drug development. Till now, there have been 11 TLRs identified in mammals and categorized depending on their respective

pathogen-associated molecular pattern (PAMP) ligands and diverse cellular positions,¹⁶ among which TLR2 is one of the most thoroughly studied receptors.

TLR2 forms heterodimers with TLR1 or TLR6, involving the recognition of PAMPs from various pathogens bacteria, fungi and other hosts,¹⁶ including substance likes Lipoprotein/lipopeptides, Peptidoglycan, Lipoteichoic acid, Glycoinositol, Phospholipids and so on.⁴ Currently, several immunomodulators of TLR2 have been developed as follows: Pam₂CSK₄, Pam₃CSK₄, CU-T12-9, BLP, MALP-2, SMP-105 as agonists, and OPN-305, CU-CPT22, E567, SSL-3 as antagonists and the others are in studying.^{17–27} However, none of the above compounds have been put into clinical practice. Thus, a novel TLR2-selective antagonist with high inhibition activity as well as low toxicity still needs to be developed emergently.

2. Design rationale

As we know that as a family of highly conservative type I transmembrane receptors, TLRs include three constituent portions: leucine-rich repeats' (LRRs) extracellular domain that involves directly the recognition of pathogen-associated molecular patterns; transmembrane domain and intracellular Toll-interleukin 1 (IL-1) receptor (TIR) domains, which are pivotal to signaling.⁴ Targeting

* Corresponding authors.

E-mail addresses: Kchennju@hotmail.com (K. Chen), chengk@smu.edu.cn (K. Cheng).

^c These three authors equally contributed to this paper.

at the BB-loop region of TIR domains, Mistry et al.²⁸ employed the computer-aided drug design (CADD) technology to screen the FDA for approved 1 million small molecules library and finally found a potential TLR2 inhibition (**C29**). Further evaluation found that it can specifically block the interaction of TLR2 and MyD88 protein, thereby inhibiting both the mouse and human TLR2/1 and TLR2/6 signaling pathways. Compound **C29** could consistently decrease Pam₃CSK₄ or Pam₂CSK₄-induced IL-8 mRNA by more than 50 percent, as well as mentioning its substrate, *o*-vanillin works. Therefore, we were wondering whether we can study the structure-activity relationship (SAR) of **C29** and expected to find the optimized structure. So, we described a series of **C29** derivatives which contained aromatic aldehydes (twelve A moiety substrates) and aromatic primary amine (eleven B moiety substrates) (Fig. 1) guided by the computer simulation and theory of bioisosterism. From the docking results of **C29** with above-mentioned BB-loop of TLR2 TIR domain (pdb: 1FYW) (Fig. S1), we got the hypothesis that the 2-hydroxyl on the aromatic aldehydes might be a potent binding site as there were small molecule-protein interactions observed. Meanwhile, we also found that a large gap between B moiety and the protein were existed, which probably indicated some large or rigid groups were tolerant in this region (Fig. S2). In addition, the polarity, steric effect, fat-solubility and electronegativity of the compounds were taken into account in designing the TLR2 inhibitors (Table. S1). Further, the derivatives of Schiff base have various pharmacological actions such as anti-inflammatory, antiviral, antibacterial and antifungal properties.²⁹ The synthetic routes for the novel TLR2 inhibitors were outlined in Fig. 1.

3. Results and discussion

These potential TLR2 antagonists were synthesized by condensation of 1:1 M ratio of aromatic aldehydes and aromatic primary amine in anhydrous methanol at 60 °C (Fig. 1B). Finally 50 potential TLR2 inhibitors were prepared in 80–90% yield. All targeted compounds were test for their TLR2 signaling pathway inhibition by a secreted embryonic alkaline phosphatase (SEAP) NF-κB reporter gene in HEK-Blue hTLR2 cells. To monitor the activation of NF-κB, the TLR2 agonist Pam₃CSK₄ was used as the positive control.

3.1. Structure-activity relationship study

Initially, we wondered whether the *N*-benzylideneaniline scaffold was essential for inhibitory hTLR2 bioactivity. So we intro-

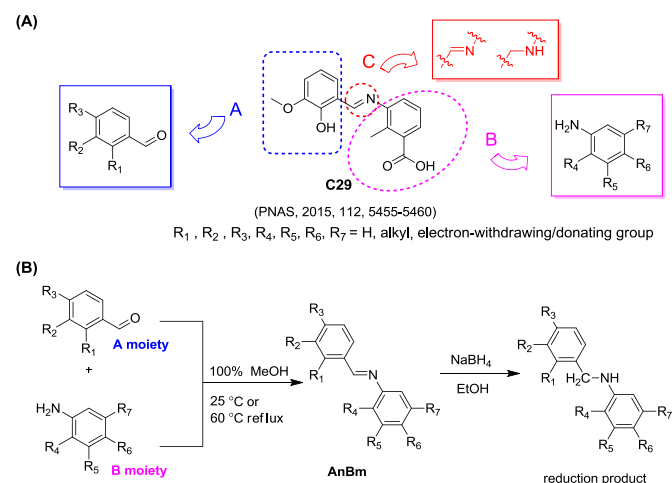


Fig. 1. General idea for the design (A) and synthetic route of the *N*-benzylideneaniline derivatives as TLR2 inhibitors (B).

duced several different aromatic or aliphatic groups and their SEAP signaling results were illustrated in Table 1. Regrettably, except **2**, **9** (with –OH at R₆ position), all of these derivatives showed negative inhibitory activity in HEK-blue hTLR2 cells, indicating the importance of the *N*-benzylideneaniline core structure. Thus, the following derivatives were developed base on this core and their bioactivity results were given in Table 2 and Fig. S3.

To confirm our hypothesis about –OH function in R₁ position, compound **21–28** were designed by either removing or methylating the hydroxy group. The experiment results indicated that removing the –OH decreased the potency significantly, which illustrated that it was critical to the activity, which also consisted with the docking result that the hydroxyl in R₁ position formed two visible hydrogen bonds with TIR domain (Fig. S1). In addition, from negligible inhibition of **21–27**, we can infer that changing the R₃ position's electronic density has no significant impact on inhibitory activity. Compared with **29** and **30**, we found that the inhibitory activity had a slight decrease when changing the methoxy (**29/C29**) to ethoxy group (**30**) at R₂ position. It required our attention that addition –OH in R₆ may play an important role in inhibitory effect. As shown in compounds **2**, **9**, **14**, **31**, **32**, **33** and **34**, which have the same B moiety, this series of compounds tended to exhibit strong inhibitory activity and it may because of the interaction between this –OH and other important residues of TLR2-TIR domain.

As mentioned previously, large gap between B moiety and the protein existed, so we introduced some big substitutions in this part. The acetophenone substitution in R₄ position (**35/SMU-AOB13**, **36**), and the phenyl substitution at R₆ position (**40**, **46**) can significantly improve the activity. These results indicated that the big/rigid substitutions on B part were tolerant and helpful for the bioactivity. In **35** (**SMU-AOB13**), the inhibitory effect was 95.06% at 50 μM, a remarkable increase compared with **C29** (51.77% inhibition at 50 μM).

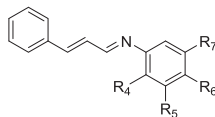
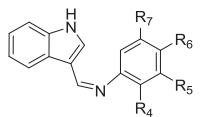
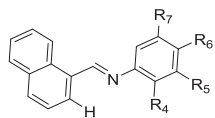
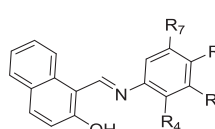
According to previous studies of Mistry,²⁸ the BB loop P681H mutation in hTLR2 plays an important role in recruiting downstream signaling. Interestingly, the docking result of **36** shows that its lowest energy conformation bears a striking resemblance to **SMU-AOB13**, the distinction is simply that the chlorine atoms of **SMU-AOB13** happens to cross over I680 and are closer to P681, so it can lead to some interaction between halogen and residues of protein, preventing P681 from triggering downstream signaling, which can explain why **SMU-AOB13**'s inhibitory activity is much better than that of **36** (Fig. 2). Further dose-dependent assay results indicated that the IC₅₀ of SMU-AOB13 was 18.21 ± 0.87 μM (Fig. 3A) and this inhibition effect was better than **C29** and the negative control **15**. What's more, to verify the biological activity after C=N been reduction, we synthesized compound **HAOB13**. The test results showed that although there has been a substantial activity decline after reduction, but **HAOB13** still maintain a certain effect (Fig. 3B).

After the SAR, we got an optimal compound **SMU-AOB13**, and then we evaluated its toxicity, downstream signal inhibition and effect on the target protein TLR2.

3.2. In vitro cytotoxicity studies

At the same time, the toxicity of these compounds were evaluated by a MTT colorimetric method. From the MTT data (Fig. 4) we can confirm that **SMU-AOB13** had no cytotoxicity at concentration up to 100 μM. Considering compound **SMU-AOB13** having the lowest IC₅₀, high inhibitory activity (95.06%), low toxicity, as well as appropriate molecular weight, it might own the higher drug-like potential ability. Thus, compound **SMU-AOB13** was picked out to evaluate its selectivity and other biophysical potential.

Table 1
Derivative 1–20 inhibition of SEAP signaling in HEK-blue hTLR2 cells.

Comd	Generic structure	R4	R5	R6	R7	Inhibition (%) ^a		
						25 μM	50 μM	
1	 derivative I	–CH ₃	–COOH	–H	–H	1.74	14.45	
2		–H	–H	–OH	–H	27.54	95.78	
3		–H	–H	–OCH ₃	–H	3.99	15.06	
4		–H	–H	–C ₆ H ₅	–H	5.63	3.10	
5	 derivative II	–CH ₃	–COOH	–H	–H	2.39	2.58	
6		–H	–H	–OCH ₃	–H	2.11	0	
7		–COOH	–H	–H	–CF ₃	0.33	5.77	
8		–H	–H	–C ₆ H ₅	–H	2.35	3.80	
9	 derivative III	–H	–H	–OH	–H	44.01	98.76	
10		–H	–H	–OCH ₃	–H	5.21	1.97	
11		–H	–H	–C ₆ H ₅	–H	0	0	
12	 derivative IV	–CH ₃	–COOH	–H	–H	0	0	
13			–H	–H	–H	–H	3.09	22.88
14		–H	–H	–OH	–H	0	0	
15		–H	–COOH	–H	–H	0	0	
16		–COOH	–CH ₃	–H	–H	0	0	
17		–H	–H	–OCH ₃	–H	3.66	0	
18		–COOH	–H	–H	–CF ₃	2.53	0	
19		–H	–H	–C ₆ H ₅	–H	5.35	1.41	
20		–H	–H	–H	–H	2.72	0	

^a Each compound was tested in triplicate.

3.3. Specificity studies

As mentioned above that TLR family can recognize a large range of ligands, so we performed a selectivity examination to investigate whether **SMU-AOB13** could specifically inhibit TLR2 signaling. The candidates included TLR1/2, TLR2/6, and TLR3, and their native ligands were Pam₃CSK₄, Pam₂CSK₄ and Poly I:C, respectively. A dose of 25 μM **SMU-AOB13** was added to the HEK series cells and then tested the stimulation of SEAP signaling. As shown in Fig. 5A, both TLR1/2 and TLR2/6 were decreased, which had no influence on TLR3, which suggested that **SMU-AOB13** is a certain specificity antagonist of TLR2.

3.4. Downstream signaling evaluation

Inducible nitric oxide synthase (iNOS) is responsible for the production of NO which can blocks phosphorylation and subsequent activation of IL-2 receptor-associated proteins, playing a major role in mediating immunosuppressive effects. TLR2-related cellular iNOS test in Raw 264.7 macrophage cells showed 40 μM **SMU-AOB13** decreased more than 70% inhibition than positive control (Fig. 5B). With the dose increasing, we observed **SMU-AOB13** can suppress Pam₃CSK₄-induced SEAP signaling as well as Pam₂CSK₄-induced one in HEK-Blue hTLR2 cells, which indicate **SMU-AOB13** through inhibit TLR2 to downregulate the TLR1/2 and TLR2/6 signaling pathway (Fig. 5B). This result also was observed in the Western blot experiment, which showed that 10 μM **SMU-AOB13** suppressed the expression of TLR2 protein by about 50% with anti-hTLR2 as the primary antibody (Fig. 5C). Meanwhile, Elisa data in human peripheral blood mononuclear cells (PBMC) showed that **SMU-AOB13** can dose dependently decrease the Pam₃CSK₄-triggered

TNF-α signaling, with 10 μM **SMU-AOB13** almost inhibiting 90% TNF-α signaling (Fig. 5D).

4. Conclusions

In conclusion, based on the previous research and guided by the CADD technology, a series of Schiff base derivatives have been designed and synthesized. Then, we made sense of the SAR discussion of these 50 compounds in human HEK-Blue TLR2 cells. Compared with lead compound C29/29, we developed a new compound **SMU-AOB13** with the most activated potential. And subsequent experiments greatly confirmed that **SMU-AOB13** had low toxicity and specific selectivity in TLR2. This can be further observed in the protein immunoblot assay which indicated that **SMU-AOB13** could efficiently downregulate the TLR2 protein. Moreover, **SMU-AOB13** can both work in murine Raw 264.7 macrophage cells and human PBMC cells to inhibit the inflammatory cytokines, including NO and TNF-α, respectively. In a manner of speaking, our study has provided a kind of potential novel small molecular, drug-like antagonist targeted at TLR2, which might be further explored involving some diseases associated with inflammation or tumor.

5. Experimental section

5.1. Chemistry

5.1.1. Materials and methods

All reagents were obtained from commercial sources and used without further purification. Reactions were followed by analytical

Table 2
Derivative 21–50 inhibition of SEAP signaling in HEK-blue hTLR2 cells.

Compds	Structure	Inhibition (%) ^a		Compds	structure	Inhibition (%) ^a	
		25 μ M	50 μ M			25 μ M	50 μ M
21		0	0	36		1.86	30.03
22		0.99	1.61	37		0	0
23		0	0	38		0	23.66
24		0	0	39		3.77	45.64
25		2.39	0	40		23.31	75.30
26		7.27	0.28	41		35.53	70.71
27		5.07	0.75	42		6.93	19.40
28		0	0	43		2.39	27.75
29		14.90	51.77	44		8.33	35.24
30		5.43	38.00	45		24.18	64.14
31		14.95	91.12	46		3.59	48.97
32		0.74	56.41	47		5.00	9.05
33		5.77	75.73	48		15.00	21.23
34		7.51	62.69	49		17.03	44.86
35 (SMU-A0B13)		66.84	95.06	50		0	19.21

^a Each compound was tested in triplicate.

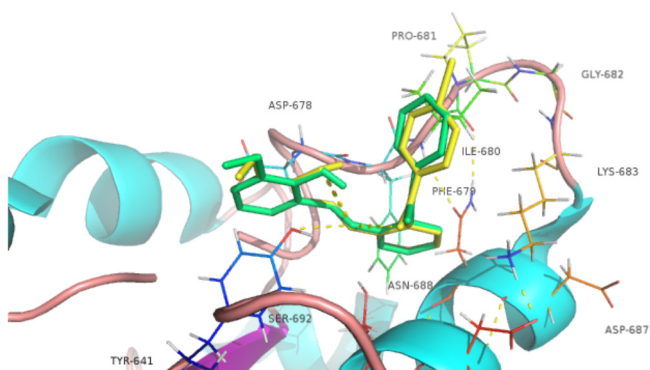


Fig. 2. The docking results between **SMU-A0B13**, **36** and BB-loop of TLR2-TIR domain. A ribbon presentation of protein and a stick representation of molecule were shown in this picture. The green one is **36** and the yellow one is **SMU-A0B13**.

thin layer chromatography (TLC), performed on pre-coated TLC plates. Flash column chromatography was performed on silica gel (300–400 mesh). The ¹H NMR spectra were obtained on AVANCE III 400 MHz (Bruker) spectrometer. Chemical shift (δ) was reported in parts per million (ppm) with TMS as an internal standard and coupling constants (J) were expressed in hertz (Hz). Low-resolution mass spectra ESI-MS were recorded on a Waters ZQ 4000 apparatus. High resolution mass spectra were performed on a Bruker Apex Qe 7T mass spectrometer.

The general condensation reaction to form Schiff base underwent addition–elimination procedure. To a vial, 1 equiv. (1 mmol) of aromatic aldehyde (A moiety) and 1 equiv. of aromatic primary amine (B moiety) were added and dissolved in 6 mL of absolute methanol. After heating and stirring at 60 °C for 3 h (or longer based on TLC), the mixture was set for 48–72 h to generate the solid Schiff base. Collecting the crystal from the solvent and checked with TLC, if aromatic aldehyde or aromatic primary amine

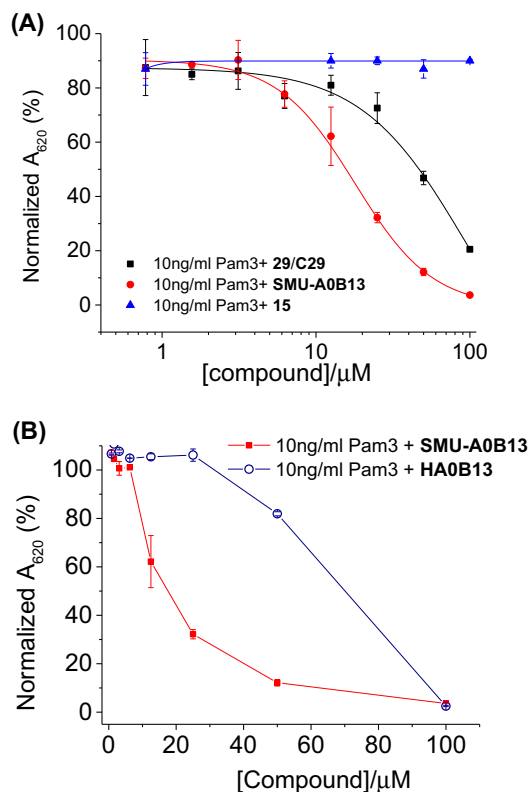


Fig. 3. The dose-dependent inhibition of SEAP signaling triggered by Pam₃SCK₄. (A) The experiment shows SMU-A0B13's inhibitory effect is better than C29, and compound 15 is a negative control. (B) The experiment shows SMU-A0B13's inhibitory effect is better than HA0B13.

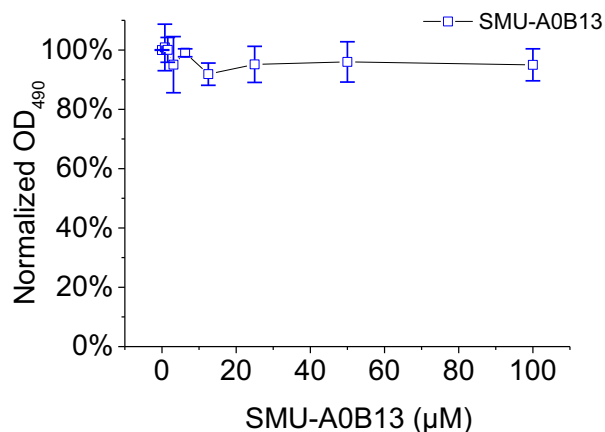


Fig. 4. Cytotoxicity of SMU-A0B13 by MTT colorimetric method.

presented, removing them by column chromatography with 1:4 ethyl acetate: petroleum ether to obtain pure product (80–90%).

5.1.1.1. 2-methyl-3-((3-phenylallylidene)amino)benzoic acid (1). ¹H NMR (400 MHz, DMSO) δ 12.89 (s, 1H), 8.27 (s, 1H), 7.69 (s, 2H), 7.60 (s, 1H), 7.45 (s, 4H), 7.29 (s, 1H), 7.21 (d, *J* = 7.1 Hz, 1H), 7.11 (s, 1H), 2.45 (s, 3H). ¹³C NMR (101 MHz, DMSO) δ 169.57, 162.87, 152.26, 144.92, 135.77, 132.75, 132.05, 130.07, 129.36, 128.76, 128.07, 127.12, 126.76, 121.32, 15.30. HRMS (ESI): *m/z* calcd for C₁₇H₁₅NO₂ [M+H]⁺ 266.1176, found 266.1177.

5.1.1.2. 4-((3-Phenylallylidene)amino)phenol (2). ¹H NMR (400 MHz, DMSO) δ 9.50 (s, 1H), 8.39 (s, 1H), 7.66 (s, 2H), 7.40 (m, 3H),

7.26 (s, 1H), 7.14 (d, *J* = 8.7 Hz, 3H), 6.80 (s, 2H). ¹³C NMR (101 MHz, CDCl₃) δ 164.35, 157.23, 141.61, 139.24, 135.85, 129.27, 128.45, 126.53, 123.96, 120.34, 118.42. ESI-MS: *m/z* calcd for C₁₅H₁₃NO [M+H]⁺ 224.3, found 224.1.

5.1.1.3. N-(4-methoxyphenyl)-3-phenylprop-2-en-1-imine (3). ¹H NMR (400 MHz, DMSO) δ 8.43 (d, *J* = 8.8 Hz, 1H), 7.66 (d, *J* = 7.2 Hz, 2H), 7.43 (s, 4H), 7.24 (d, *J* = 6.8 Hz, 2H), 7.14 (m, 1H), 6.97 (d, *J* = 8.8 Hz, 2H), 3.78 (s, 3H). ¹³C NMR (101 MHz, CDCl₃) δ 164.37, 160.43, 141.21, 139.39, 135.83, 128.10, 126.92, 126.23, 123.76, 120.44, 116.29, 56.34. ESI-MS: *m/z* calcd for C₁₆H₁₅NO [M+H]⁺ 238.3, found 237.7.

5.1.1.4. N-(3-Phenylallylidene)-[1,1'-biphenyl]-4-amine (4). ¹H NMR (400 MHz, DMSO) δ 8.50 (s, 1H), 7.71 (s, 6H), 7.50–7.41 (m, 5H), 7.39 (s, 2H), 7.33 (s, 2H), 7.20 (d, *J* = 7.1 Hz, 1H). ¹³C NMR (101 MHz, DMSO) δ 162.36, 151.12, 144.74, 140.04, 138.24, 135.92, 130.06, 129.41, 128.92, 128.04, 127.90, 127.77, 126.89, 121.98 (s). ESI-MS: *m/z* calcd for C₂₁H₁₇N [M+H]⁺ 284.4, found 284.2.

5.1.1.5. 3-(((1H-Indol-3-yl)methylene)amino)-2-methylbenzoic acid (5). ¹H NMR (400 MHz, DMSO) δ 12.13 (s, 1H), 9.94 (s, 1H), 8.28 (s, 1H), 8.11 (s, 1H), 7.51 (s, 1H), 7.25 (m, 2H), 6.92 (m, 2H), 6.77 (dd, *J* = 7.6, 1.5 Hz, 1H), 5.02 (s, 1H), 2.19 (s, 3H). ¹³C NMR (101 MHz, DMSO) δ 185.40, 170.67, 147.81, 138.79, 137.50, 133.00, 126.04, 124.57, 123.89, 122.57, 121.28, 121.16, 118.62, 117.78, 117.17, 112.84, 14.36. ESI-MS: *m/z* calcd for C₁₇H₁₄N₂O₂ [M+H]⁺ 279.3, found 279.1.

5.1.1.6. N-((1H-Indol-3-yl)methylene)-4-methoxyaniline (6). ¹H NMR (400 MHz, DMSO) δ 11.70 (s, 1H), 8.71 (s, 1H), 8.39 (s, 1H), 7.96 (s, 1H), 7.49 (s, 1H), 7.21 (d, *J* = 8.8 Hz, 2H), 7.17 (s, 1H), 6.96 (d, *J* = 8.9 Hz, 2H), 3.77 (s, 3H). ¹³C NMR (101 MHz, DMSO) δ 157.23, 154.11, 146.56, 137.54, 133.23, 125.19, 123.11, 122.27, 122.12, 121.12, 115.54, 114.76, 112.32, 55.66. ESI-MS: *m/z* calcd for C₁₆H₁₄N₂O [M+H]⁺ 251.3, found 251.2.

5.1.1.7. 2-(((1H-Indol-3-yl)methylene)amino)-4-(trifluoromethyl)benzoic acid (7). ¹H NMR (400 MHz, DMSO) δ 9.12 (s, 1H), 8.34 (s, 1H), 8.20 (d, *J* = 7.5 Hz, 2H), 8.03 (s, 1H), 7.87 (d, *J* = 8.2 Hz, 1H), 7.67 (d, *J* = 8.2 Hz, 1H), 7.61 (d, *J* = 6.7 Hz, 1H), 7.34 (s, 2H). ¹³C NMR (101 MHz, DMSO) δ 185.38, 169.09, 151.76, 138.89, 138.15, 137.45, 132.99, 132.31, 124.52, 123.87, 122.94, 122.53, 121.23, 120.98, 118.57, 113.46, 112.83. HRMS (ESI): *m/z* calcd for C₁₇H₁₁N₂O₂ F₃ [M+H]⁺ 333.0845, found 333.0845.

5.1.1.8. N-((1H-Indol-3-yl)methylene)-[1,1'-biphenyl]-4-amine (8). ¹H NMR (400 MHz, DMSO) δ 11.79 (s, 1H), 8.78 (s, 1H), 8.40 (s, 1H), 8.03 (s, 1H), 7.70 (d, *J* = 7.8 Hz, 4H), 7.47 (s, 3H), 7.34 (s, 3H), 7.22 (s, 2H). ¹³C NMR (101 MHz, DMSO) δ 155.73, 152.89, 140.29, 137.66, 136.79, 134.08, 129.34, 127.79, 127.47, 126.74, 125.25, 123.32, 122.36, 121.82, 121.40, 115.59, 112.47. ESI-MS: *m/z* calcd for C₂₁H₁₆N₂ [M+H]⁺ 297.4, found 297.7.

5.1.1.9. 4-((Naphthalen-1-ylmethylene)amino)phenol (9). ¹H NMR (400 MHz, DMSO) δ 9.54 (s, 1H), 9.23 (s, 1H), 9.21 (s, 1H), 8.15 (s, 1H), 8.07 (s, 1H), 8.02 (s, 1H), 7.63 (s, 3H), 7.32 (s, 2H), 6.84 (s, 2H). ¹³C NMR (101 MHz, DMSO) δ 157.33, 156.83, 143.58, 133.97, 131.88, 131.64, 131.27, 129.91, 129.04, 127.71, 126.63, 125.88, 125.00, 123.08, 116.19. ESI-MS: *m/z* calcd for C₁₇H₁₃NO [M+H]⁺ 248.3, found 248.5.

5.1.1.10. 4-Methoxy-N-(naphthalen-1-ylmethylene)aniline (10). ¹H NMR (400 MHz, DMSO) δ 9.24 (d, *J* = 11.1 Hz, 2H), 8.17 (d, *J* = 7.0 Hz, 1H), 8.10 (s, 1H), 8.05 (s, 1H), 7.65 (s, 3H), 7.44 (s, 2H), 7.04 (s, 2H). ¹³C NMR (101 MHz, DMSO) δ 158.52, 158.45, 145.04,

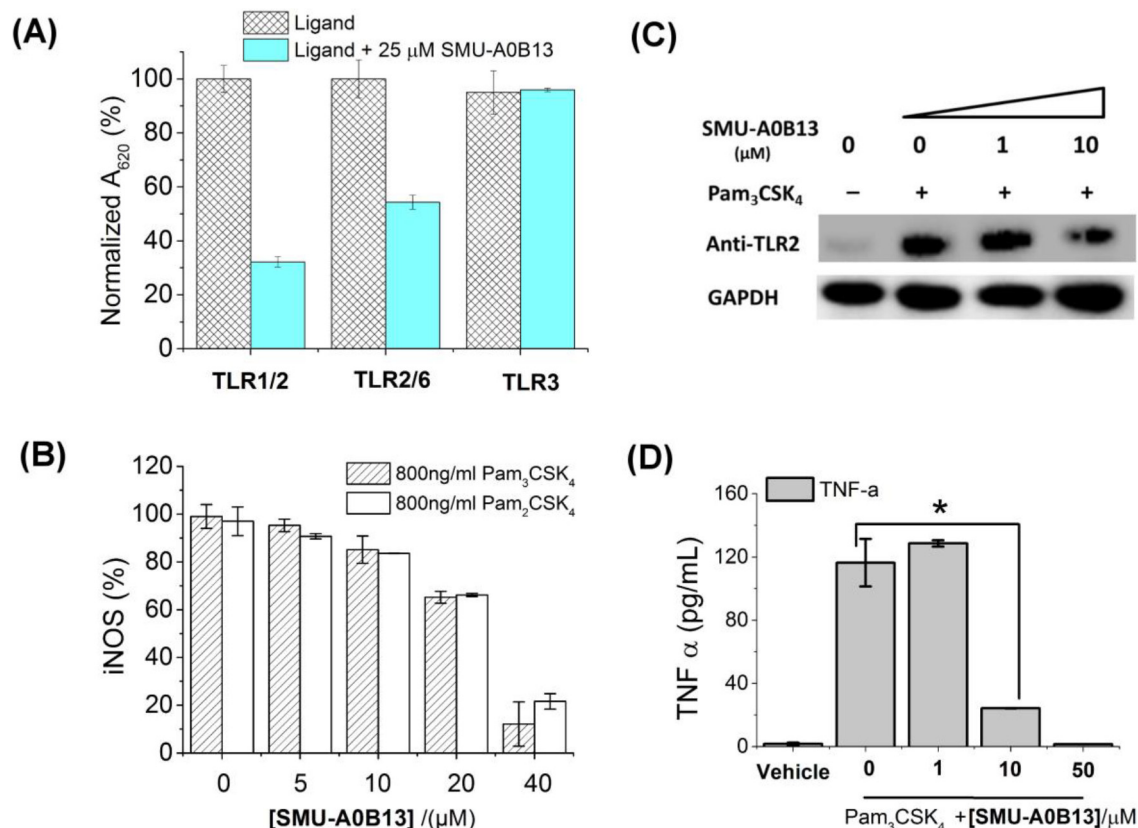


Fig. 5. The influence of SMU-A0B13 in the TLR2 signaling pathway. (A) The SEAP specificity experiment showed SMU-A0B13 can inhibit both TLR1/2 and TLR2/6, not TLR3. The ligand for TLR1/2, TLR2/6, and TLR3 are 10 ng/mL Pam₃CSK₄, 10 ng/mL Pam₂CSK₄ and 10 μg/mL Poly I:C, respectively. (B) The iNOS inhibition by SMU-A0B13 in Raw 264.7 macrophage cells. Pam₃CSK₄ and Pam₂CSK₄ are the ligands for TLR1/2 and TLR2/6. (C) The Western Blot experiment indicated SMU-A0B13 can inhibit the Pam₃CSK₄ (400 ng/mL) upregulated TLR2 in HEK-Blue hTLR2 cells. (D) ELISA assay showed SMU-A0B13 can inhibit the TNF-α signaling which activated by Pam₃CSK₄ in human PBMC cells. Data shown are mean ± SD of representative data of three independent experiments. * P < 0.05.

133.97, 131.88, 131.74, 131.28, 130.20, 129.07, 127.79, 126.67, 125.87, 125.00, 122.98, 114.86, 55.74. ESI-MS: *m/z* calcd for C₁₈H₁₅NO [M+H]⁺ 262.3, found 261.7.

5.1.1.11. *N*-(Naphthalen-1-ylmethylene)-[1,1'-biphenyl]-4-amine (**11**). ¹H NMR (400 MHz, DMSO) δ 9.31 (s, 1H), 9.27 (s, 1H), 8.22 (s, 1H), 8.14 (s, 1H), 8.08 (s, 1H), 7.78 (d, *J* = 8.5 Hz, 2H), 7.74 (d, *J* = 7.2 Hz, 2H), 7.72–7.62 (m, 3H), 7.57 (s, 1H), 7.41 (m, 2H), 7.39 (s, 1H). ¹³C NMR (101 MHz, DMSO) δ 160.85, 151.49, 140.06, 138.30, 133.98, 132.41, 131.48, 131.32, 130.89, 129.38, 129.14, 127.99, 127.90, 127.76, 126.90, 126.77, 125.88, 125.02, 122.25. ESI-MS: *m/z* calcd for C₂₃H₁₇N [M+H]⁺ 308.4, found 307.9.

5.1.1.12. 3-(((2-Hydroxynaphthalen-1-yl)methylene)amino)-2-methylbenzoic acid (**12**). ¹H NMR (400 MHz, DMSO) δ 15.77 (s, 1H), 13.10 (s, 1H), 9.65 (s, 1H), 8.54 (s, 1H), 7.97 (s, 1H), 7.91 (s, 1H), 7.84 (s, 1H), 7.67 (s, 1H), 7.57 (s, 1H), 7.41 (m, 2H), 7.09 (s, 1H), 2.58 (s, 3H). ¹³C NMR (101 MHz, DMSO) δ 169.71, 169.44, 157.43, 145.23, 137.21, 133.47, 133.43, 130.79, 129.42, 128.54, 127.83, 127.21, 127.17, 124.00, 122.02, 122.00, 120.88, 109.38, 15.17. HRMS (ESI): *m/z* calcd for C₁₉H₁₅NO₃ [M+H]⁺ 306.1125, found 306.1126.

5.1.1.13. (4-Chlorophenyl)2-(((2-hydroxynaphthalen-1-yl)methylene)amino)phenyl)methanone (**13**). ¹H NMR (400 MHz, DMSO) δ 14.31 (s, 1H), 9.64 (s, 1H), 8.49 (d, *J* = 8.6 Hz, 1H), 7.94 (s, 2H), 7.77 (t, *J* = 11.0 Hz, 4H), 7.63 (s, 2H), 7.53 (s, 2H), 7.47 (s, 1H), 7.38 (s, 1H), 6.97 (d, *J* = 9.1 Hz, 1H). ¹³C NMR (101 MHz, DMSO) δ 195.84, 166.94, 158.62, 144.93, 139.06, 136.95, 135.93, 133.20,

132.92, 132.58, 131.90, 129.46, 129.39, 129.33, 128.52, 127.47, 126.68, 124.13, 121.14, 121.03, 119.96, 109.62. ESI-MS: *m/z* calcd for C₂₄H₁₆ClNO₂ [M+H]⁺ 386.8, found 386.8.

5.1.1.14. 1-(((4-Hydroxyphenyl)imino)methyl)naphthalen-2-ol (**14**). ¹H NMR (400 MHz, DMSO) δ 16.07 (s, 1H), 9.69 (s, 1H), 9.61 (d, *J* = 4.4 Hz, 1H), 8.48 (d, *J* = 8.5 Hz, 1H), 7.91 (s, 1H), 7.79 (d, *J* = 4.1 Hz, 1H), 7.51 (d, *J* = 8.7 Hz, 3H), 7.34 (s, 1H), 7.02 (d, *J* = 9.1 Hz, 1H), 6.88 (d, *J* = 8.7 Hz, 2H). ¹³C NMR (101 MHz, DMSO) δ 169.30, 157.07, 154.24, 136.23, 136.15, 133.45, 129.33, 128.25, 127.04, 123.59, 122.41, 122.23, 120.63, 116.54, 108.92. ESI-MS: *m/z* calcd for C₁₇H₁₃NO₂ [M+H]⁺ 264.3, found 264.1.

5.1.1.15. 3-(((2-Hydroxynaphthalen-1-yl)methylene)amino)benzoic acid (**15**). ¹H NMR (400 MHz, DMSO) δ 15.63 (d, *J* = 3.7 Hz, 1H), 13.20 (s, 1H), 9.74 (d, *J* = 2.7 Hz, 1H), 8.55 (d, *J* = 8.5 Hz, 1H), 8.08 (s, 1H), 7.97 (d, *J* = 9.2 Hz, 1H), 7.89 (t, *J* = 9.2 Hz, 2H), 7.82 (d, *J* = 7.9 Hz, 1H), 7.63 (t, *J* = 7.8 Hz, 1H), 7.57 (s, 1H), 7.38 (s, 1H), 7.06 (d, *J* = 9.2 Hz, 1H). ¹³C NMR (101 MHz, DMSO) δ 169.97, 167.34, 157.40, 145.21, 137.31, 133.49, 132.75, 130.28, 129.39, 128.51, 127.54, 127.21, 125.24, 124.00, 122.13, 121.87, 120.99, 109.18. ESI-MS: *m/z* calcd for C₁₈H₁₃NO₃ [M+H]⁺ 292.3, found 292.1.

5.1.1.16. 2-(((2-Hydroxynaphthalen-1-yl)methylene)amino)-6-methylbenzoic acid (**16**). ¹H NMR (400 MHz, DMSO) δ 15.11 (s, 1H), 13.49 (s, 1H), 9.70 (s, 1H), 8.54 (d, *J* = 8.6 Hz, 1H), 8.01 (s, 1H), 7.87 (s, 1H), 7.69 (s, 1H), 7.58 (s, 1H), 7.43 (m, 2H), 7.24 (s, 1H), 7.12 (s, 1H), 2.36 (s, 3H). ¹³C NMR (101 MHz, DMSO) δ 169.81, 166.40, 158.67, 143.29, 136.62, 135.27, 133.24, 130.95,

130.33, 129.41, 128.58, 128.51, 127.51, 124.08, 121.06, 120.98, 116.57, 109.62, 19.51. HRMS (ESI): m/z calcd for $C_{19}H_{15}NO_3$ $[M+H]^+$ 306.1125, found 306.1126.

5.1.1.17. 1-(((4-Methoxyphenyl)imino)methyl)naphthalen-2-ol (**17**). 1H NMR (400 MHz, DMSO) δ 15.98 (s, 1H), 9.65 (s, 1H), 8.51 (s, 1H), 7.91 (s, 1H), 7.79 (s, 1H), 7.63 (d, J = 8.9 Hz, 2H), 7.55 (s, 1H), 7.35 (s, 1H), 7.09–7.01 (m, 3H), 3.82 (s, 3H). ^{13}C NMR (101 MHz, $CDCl_3$) δ 171.04, 159.11, 153.88, 144.36, 133.05, 132.41, 129.10, 128.02, 126.84, 129.96, 122.13, 120.56, 118.63, 115.65, 108.52, 55.83. ESI-MS: m/z calcd for $C_{18}H_{15}NO_2$ $[M+H]^+$ 278.3, found 278.2.

5.1.1.18. 2-(((2-Hydroxynaphthalen-1-yl)methylene)amino)-4-(trifluoromethyl)benzoic acid (**18**). 1H NMR (400 MHz, DMSO) δ 12.00 (s, 1H), 10.82 (s, 1H), 9.53 (s, 1H), 8.50 (d, J = 8.3 Hz, 1H), 8.33 (s, 1H), 8.10 (d, J = 8.1 Hz, 1H), 7.92 (d, J = 9.3 Hz, 1H), 7.77 (d, J = 7.7 Hz, 1H), 7.69 (s, 1H), 7.55 (s, 1H), 7.36 (s, 1H), 6.92 (d, J = 8.9 Hz, 1H). ^{13}C NMR (101 MHz, DMSO) δ 193.31, 173.61, 167.25, 154.67, 144.84, 138.72, 133.96, 132.31, 129.48, 128.68, 127.22, 124.31, 123.59, 121.38, 117.02, 109.78. HRMS (ESI): m/z calcd for $C_{19}H_{12}F_3NO_3$ $[M+H]^+$ 360.0842, found 360.0844.

5.1.1.19. 1-(((1,1'-Biphenyl)-4-ylimino)methyl)naphthalen-2-ol (**19**). 1H NMR (400 MHz, DMSO) δ 15.86 (s, 1H), 9.72 (s, 1H), 8.53 (d, J = 8.5 Hz, 1H), 7.94 (d, J = 9.2 Hz, 1H), 7.82 (d, J = 8.6 Hz, 3H), 7.75 (d, J = 8.8 Hz, 4H), 7.56 (dd, J = 11.3, 4.1 Hz, 1H), 7.50 (t, J = 7.6 Hz, 2H), 7.37 (s, 2H), 7.03 (s, 1H). ^{13}C NMR (101 MHz, DMSO) δ 171.44, 155.42, 143.38, 139.69, 138.60, 137.42, 133.61, 129.43, 129.39(s), 128.18, 127.93, 127.07, 126.92, 123.90, 122.74, 121.38, 120.78, 109.03. ESI-MS: m/z calcd for $C_{23}H_{17}NO$ $[M+H]^+$ 324.4, found 325.1.

5.1.1.20. 2-(((2-Hydroxynaphthalen-1-yl)methylene)amino)phenyl(methanone) (**20**). 1H NMR (400 MHz, DMSO) δ 14.41 (s, 1H), 9.64 (s, 1H), 8.49 (s, 1H), 7.94 (s, 2H), 7.79 (s, 3H), 7.76 (s, 1H), 7.67 (t, J = 7.3 Hz, 1H), 7.55 (s, 4H), 7.46 (s, 1H), 7.38 (s, 1H), 6.96 (s, 1H). ^{13}C NMR (101 MHz, DMSO) δ 196.90, 167.20, 158.39, 144.77, 137.20, 136.93, 134.12, 133.32, 133.24, 132.36, 130.11, 129.38, 129.27, 128.52, 127.42, 126.57, 124.10, 121.16, 121.08, 119.94, 109.57. ESI-MS: m/z calcd for $C_{24}H_{17}NO_2$ $[M+H]^+$ 352.4, found 351.8.

5.1.1.21. 2-Methyl-3-((4-(trifluoromethyl)benzylidene)amino)benzoic acid (**21**). 1H NMR (400 MHz, DMSO) δ 8.14 (d, J = 8.1 Hz, 3H), 7.88 (d, J = 8.3 Hz, 3H), 6.93 (m, 1H), 6.78 (m, 1H), 2.19 (s, 3H). ^{13}C NMR (101 MHz, DMSO) δ 170.57, 166.62, 147.85, 135.01, 132.87, 130.52, 129.73, 126.02, 125.99, 121.55, 121.12, 117.67, 117.12, 14.33. HRMS (ESI): m/z calcd for $C_{16}H_{12}NO_2F_3$ $[M+H]^+$ 308.0893, found 308.0890.

5.1.1.22. 3-(((3-Methoxybenzylidene)amino)-2-methylbenzoic acid (**22**). 1H NMR (400 MHz, DMSO) δ 12.86 (s, 1H), 8.47 (s, 1H), 7.62 (d, J = 7.7 Hz, 1H), 7.54 (d, J = 7.3 Hz, 2H), 7.46 (t, J = 7.8 Hz, 1H), 7.31 (t, J = 7.8 Hz, 1H), 7.20 (d, J = 7.7 Hz, 1H), 7.17–7.11 (m, 1H), 3.84 (s, 3H), 2.48 (s, 3H). ^{13}C NMR (101 MHz, DMSO) δ 169.51, 161.13, 160.01, 151.92, 137.87, 132.67, 132.13, 130.39, 127.31, 126.80, 121.87, 121.50, 117.95, 113.40, 55.67, 15.37. HRMS (ESI): m/z calcd for $C_{16}H_{15}NO_3$ $[M+H]^+$ 270.1125, found 270.1126.

5.1.1.23. 3-Amino-5-((4-hydroxy-3-methoxybenzylidene)amino)benzoic acid (**23**). 1H NMR (400 MHz, DMSO) δ 9.23 (s, 1H), 6.83 (s, 1H), 6.73 (s, 1H), 6.59 (s, 1H), 6.25 (s, 1H), 6.20 (s, 1H), 6.13 (s, 1H), 5.29 (s, 2H), 4.70 (s, 2H), 3.71 (s, 3H). ^{13}C NMR (101 MHz, DMSO) δ 171.63, 151.53, 147.94, 147.68, 144.00, 127.57, 127.42,

122.53, 120.74, 115.92, 112.50, 105.27, 97.50, 81.68, 56.03. ESI-MS: m/z calcd for $C_{15}H_{14}N_2O_4$ $[M+H]^+$ 287.3, found 287.1.

5.1.1.24. 2-Methoxy-4-(((4-methoxyphenyl)imino)methyl)phenol (**24**). 1H NMR (400 MHz, DMSO) δ 9.67 (s, 1H), 8.46 (s, 1H), 7.51 (s, 1H), 7.31 (d, J = 8.1 Hz, 1H), 7.23 (d, J = 8.7 Hz, 2H), 6.96 (d, J = 8.7 Hz, 2H), 6.88 (d, J = 8.1 Hz, 1H), 3.85 (s, 3H), 3.77 (s, 3H). ^{13}C NMR (101 MHz, $CDCl_3$) δ 181.21, 153.34, 152.57, 147.99, 132.23, 125.87, 124.14, 117.36, 115.17, 103.61, 102.44, 58.42, 55.81. ESI-MS: m/z calcd for $C_{15}H_{15}NO_3$ $[M+H]^+$ 258.3, found 258.1.

5.1.1.25. 4-(((1,1'-Biphenyl)-4-ylimino)methyl)-2-methoxyphenol (**25**). 1H NMR (400 MHz, DMSO) δ 9.77 (s, 1H), 8.52 (s, 1H), 7.71 (d, J = 8.4 Hz, 4H), 7.56 (s, 1H), 7.47 (s, 2H), 7.36 (m, 4H), 6.92 (s, 1H), 3.87 (s, 3H). ^{13}C NMR (101 MHz, DMSO) δ 160.53, 151.55, 150.75, 148.45, 140.10, 137.61, 129.35, 128.36, 127.81, 127.63, 126.81, 124.68, 121.96, 115.81, 110.84, 55.97. ESI-MS: m/z calcd for $C_{20}H_{17}NO_2$ $[M+H]^+$ 304.4, found 304.7.

5.1.1.26. 4-Methoxy-N-(4-(trifluoromethyl)benzylidene)aniline (**26**). 1H NMR (400 MHz, DMSO) δ 8.78 (s, 1H), 8.12 (s, 2H), 7.88 (s, 2H), 7.38 (d, J = 8.9 Hz, 2H), 7.02 (d, J = 8.9 Hz, 2H), 3.80 (s, 3H). ^{13}C NMR (101 MHz, $CDCl_3$) δ 160.05, 159.12, 144.38, 139.74, 133.37, 129.52, 125.26, 124.16, 122.13, 115.61, 55.80. ESI-MS: m/z calcd for $C_{15}H_{12}F_3NO$ $[M+H]^+$ 280.3, found 280.1.

5.1.1.27. N-(4-(Trifluoromethyl)benzylidene)-[1,1'-biphenyl]-4-amine (**27**). 1H NMR (400 MHz, DMSO) δ 8.84 (s, 1H), 8.17 (s, 2H), 7.92 (s, 2H), 7.76 (s, 2H), 7.71 (s, 2H), 7.47 (m, 4H), 7.38 (s, 1H). ^{13}C NMR (101 MHz, $CDCl_3$) δ 158.29, 150.41, 140.47, 139.63, 139.30, 129.00, 128.87, 127.98, 127.40, 126.98, 125.78, 125.75, 121.47. HRMS (ESI): m/z calcd for $C_{20}H_{14}F_3N$ $[M+H]^+$ 326.1156, found 326.1155.

5.1.1.28. N-(3-Methoxybenzylidene)-[1,1'-biphenyl]-4-amine (**28**). 1H NMR (400 MHz, DMSO) δ 8.68 (s, 1H), 7.76–7.69 (m, 4H), 7.56–7.52 (m, 2H), 7.51–7.43 (m, 3H), 7.38 (d, J = 8.5 Hz, 3H), 7.13 (d, J = 8.3 Hz, 1H), 3.85 (s, 3H). ^{13}C NMR (101 MHz, DMSO) δ 160.94, 160.00, 150.95, 139.99, 138.30, 137.92, 130.36, 129.38, 127.83 (d), 126.89, 122.11, 118.21, 113.04, 55.67. HRMS (ESI): m/z calcd for $C_{20}H_{17}NO$ $[M+H]^+$ 288.1383, found 288.1386.

5.1.1.29. 3-(((2-Hydroxy-3-methoxybenzylidene)amino)-2-methylbenzoic acid (**29**). 1H NMR (400 MHz, DMSO) δ 13.07 (m, 2H), 8.85 (s, 1H), 7.67 (d, J = 7.6 Hz, 1H), 7.46 (d, J = 7.7 Hz, 1H), 7.38 (t, J = 7.7 Hz, 1H), 7.28 (d, J = 7.8 Hz, 1H), 7.16 (d, J = 7.9 Hz, 1H), 6.94 (t, J = 7.9 Hz, 1H), 3.84 (s, 3H). ^{13}C NMR (101 MHz, DMSO) δ 169.51, 161.13, 160.01, 151.88, 137.87, 132.71, 132.13, 130.39, 127.31, 126.80, 121.91, 121.58, 118.08, 113.40, 55.67, 15.29. ESI-MS: m/z calcd for $C_{16}H_{15}NO_4$ $[M+H]^+$ 286.3, found 286.1.

5.1.1.30. 3-(((3-Ethoxy-2-hydroxybenzylidene)amino)-2-methylbenzoic acid (**30**). 1H NMR (400 MHz, DMSO) δ 13.17 (s, 1H), 13.03 (s, 1H), 8.85 (s, 1H), 7.67 (d, J = 7.6 Hz, 1H), 7.47 (d, J = 7.8 Hz, 1H), 7.38 (t, J = 7.8 Hz, 1H), 7.27 (d, J = 7.7 Hz, 1H), 7.15 (d, J = 7.9 Hz, 1H), 6.92 (t, J = 7.8 Hz, 1H), 4.09 (d, J = 7.0 Hz, 2H), 1.37 (t, J = 6.9 Hz, 3H), 1.24 (s, 3H). ^{13}C NMR (101 MHz, DMSO) δ 169.43, 164.72, 151.18, 148.73, 147.48, 133.26, 132.14, 128.20, 127.09, 124.48, 121.96, 119.84, 119.10, 117.39, 64.50, 15.28, 15.18. HRMS (ESI): m/z calcd for $C_{17}H_{17}NO_4$ $[M+H]^+$ 300.1230, found 300.1228.

5.1.1.31. 2-(((4-Hydroxyphenyl)imino)methyl)-6-methoxyphenol (**31**). 1H NMR (400 MHz, DMSO) δ 13.60 (s, 1H), 9.68 (s, 1H), 8.89 (s, 1H), 7.33 (s, 2H), 7.17 (s, 1H), 7.08 (s, 1H), 6.89 (s, 1H), 6.85 (d, J = 8.7 Hz, 2H), 3.82 (s, 3H). ^{13}C NMR (101 MHz, DMSO) δ 160.75, 157.40, 150.82, 148.26, 139.42, 124.08, 123.04, 119.74,

118.82, 116.39, 115.46, 56.26. ESI-MS: m/z calcd for $C_{14}H_{13}NO_3$ [M+H]⁺ 244.3, found 244.1.

5.1.1.32. 4-((3-Methoxybenzylidene)amino)phenol (**32**). ¹H NMR (400 MHz, DMSO) δ 9.50 (s, 1H), 8.59 (s, 1H), 7.47 (s, 2H), 7.40 (d, J = 7.9 Hz, 1H), 7.19 (s, 2H), 7.06 (d, J = 7.9 Hz, 1H), 6.80 (d, J = 11.9 Hz, 2H), 3.83 (s, 3H). ¹³C NMR (101 MHz, DMSO) δ 159.55, 157.06, 156.37, 142.49, 137.94, 129.85, 122.55, 121.25, 117.11, 115.73, 112.20, 55.19. ESI-MS: m/z calcd for $C_{14}H_{13}NO_2$ [M+H]⁺ 228.3, found 227.7.

5.1.1.33. 2-Ethoxy-6-(((4-hydroxyphenyl)imino)methyl)phenol (**33**). ¹H NMR (400 MHz, DMSO) δ 13.64 (s, 1H), 9.67 (s, 1H), 8.89 (s, 1H), 7.32 (d, J = 8.7 Hz, 2H), 7.18 (d, J = 7.8 Hz, 1H), 7.07 (d, J = 9.1 Hz, 1H), 6.85 (d, J = 8.7 Hz, 3H), 4.07 (d, J = 7.0 Hz, 2H), 1.35 (s, 3H). ¹³C NMR (101 MHz, DMSO) δ 160.71, 157.42, 151.15, 147.39, 139.36, 124.25, 123.02, 119.85, 118.79, 116.85, 116.40, 64.49, 15.21. ESI-MS: m/z calcd for $C_{15}H_{15}NO_3$ [M+H]⁺ 258.3, found 258.1.

5.1.1.34. 4-(((4-Hydroxyphenyl)imino)methyl)-2-methoxyphenol (**34**). ¹H NMR (400 MHz, DMSO) δ 9.61 (s, 1H), 9.38 (s, 1H), 8.43 (s, 1H), 7.49 (s, 1H), 7.28 (d, J = 7.8 Hz, 1H), 7.12 (d, J = 8.2 Hz, 2H), 6.87 (d, J = 8.0 Hz, 1H), 6.78 (d, J = 8.2 Hz, 2H), 3.84 (s, 3H). ¹³C NMR (101 MHz, DMSO) δ 157.56, 156.16, 150.13, 148.42, 143.64, 128.78, 124.01, 122.62, 116.14, 115.79, 110.51, 55.96. ESI-MS: m/z calcd for $C_{14}H_{13}NO_3$ [M+H]⁺ 244.3, found 244.2.

5.1.1.35. (SMU-A0B13) (4-chlorophenyl)(2-((2-hydroxy-3-methoxybenzylidene)amino)phenyl)methanone (**35**). ¹H NMR (400 MHz, DMSO) δ 11.88 (s, 1H), 8.91 (s, 1H), 7.74 (d, J = 8.5 Hz, 2H), 7.69 (s, 1H), 7.60 (d, J = 8.4 Hz, 3H), 7.53–7.44 (m, 2H), 7.12 (s, 1H), 7.07 (s, 1H), 6.86 (s, 1H), 3.75 (s, 3H). ¹³C NMR (101 MHz, DMSO) δ 195.94, 164.83, 150.39, 148.12, 146.61, 139.04, 135.88, 134.43, 132.22, 131.72, 129.49, 128.68, 127.29, 124.30, 119.54, 119.32, 119.12, 116.28, 56.17. HRMS (ESI): m/z calcd for $C_{21}H_{16}ClNO_3$ [M+H]⁺ 366.0897, found 366.0895.

5.1.1.36. (2-((2-Hydroxy-3-methoxybenzylidene)amino)phenyl)(phenyl)methanone (**36**). ¹H NMR (400 MHz, DMSO) δ 11.94 (s, 1H), 8.90 (s, 1H), 7.74 (d, J = 7.3 Hz, 2H), 7.66 (s, 2H), 7.61 (s, 1H), 7.51 (m, 4H), 7.12 (s, 1H), 7.06 (s, 1H), 6.85 (s, 1H), 3.74 (s, 3H). ¹³C NMR (101 MHz, DMSO) δ 197.00, 164.80, 150.41, 148.11, 146.57, 137.12, 134.92, 134.14, 131.97, 129.91, 129.28, 128.60, 127.19, 124.34, 119.50, 119.29, 119.05, 116.16, 56.13. HRMS (ESI): m/z calcd for $C_{21}H_{17}NO_3$ [M+H]⁺ 332.1281, found 332.1285.

5.1.1.37. *N*-(2,3-Dimethoxybenzylidene)-4-methoxyaniline (**37**). ¹H NMR (400 MHz, DMSO) δ 8.79 (s, 1H), 7.61 (d, J = 7.4 Hz, 1H), 7.28 (d, J = 8.9 Hz, 2H), 7.18 (dd, J = 8.2, 4.8 Hz, 2H), 6.99 (d, J = 8.9 Hz, 2H), 3.86 (s, 3H), 3.85 (s, 3H), 3.78 (s, 3H). ¹³C NMR (101 MHz, CDCl₃) δ 158.20, 154.32, 152.76, 149.83, 145.18, 130.05, 122.36, 124.20, 118.74, 114.61, 114.27, 61.85, 55.81, 55.40. ESI-MS: m/z calcd for $C_{16}H_{17}NO_3$ [M+H]⁺ 272.3, found 272.1.

5.1.1.38. 3-((2-Hydroxy-3-methoxybenzylidene)amino)benzoic acid (**38**). ¹H NMR (400 MHz, DMSO) δ 13.16 (s, 1H), 12.96 (s, 1H), 9.03 (s, 1H), 7.92 (s, 1H), 7.89 (d, J = 7.6 Hz, 1H), 7.67 (d, J = 8.7 Hz, 1H), 7.60 (t, J = 7.7 Hz, 1H), 7.30 (d, J = 7.8 Hz, 1H), 7.16 (d, J = 7.9 Hz, 1H), 6.93 (t, J = 7.9 Hz, 1H), 3.84 (s, 3H). ¹³C NMR (101 MHz, DMSO) δ 167.36, 164.98, 150.92, 148.70, 148.32, 132.57, 130.21, 128.01, 126.40, 124.40, 122.20, 119.63, 119.11, 116.14, 56.26. ESI-MS: m/z calcd for $C_{15}H_{13}NO_4$ [M+H]⁺ 272.3, found 272.2.

5.1.1.39. 2-Methoxy-6-(((4-methoxyphenyl)imino)methyl)phenol (**39**). ¹H NMR (400 MHz, DMSO) δ 13.46 (s, 1H), 8.94 (s, 1H),

7.43 (d, J = 8.9 Hz, 2H), 7.20 (s, 1H), 7.10 (s, 1H), 7.02 (s, 2H), 6.90 (s, 1H), 3.84 (s, 3H), 3.80 (s, 3H). ¹³C NMR (101 MHz, CDCl₃) δ 160.67, 159.30, 151.65, 148.79, 141.27, 123.98, 122.69, 119.67, 118.83, 114.99, 114.80, 56.53, 55.87. ESI-MS: m/z calcd for $C_{15}H_{15}NO_3$ [M+H]⁺ 258.3, found 258.2.

5.1.1.40. 2-(((1,1'-Biphenyl)-4-ylimino)methyl)-6-methoxyphenol (**40**). ¹H NMR (400 MHz, DMSO) δ 13.27 (s, 1H), 9.04 (s, 1H), 7.77 (s, 2H), 7.71 (s, 2H), 7.52 (m, 4H), 7.39 (s, 1H), 7.26 (s, 1H), 7.14 (s, 1H), 6.93 (s, 1H), 3.84 (s, 3H). ¹³C NMR (101 MHz, DMSO) δ 163.81, 151.05, 148.36, 147.41, 139.75, 139.17, 129.40, 128.09, 127.97, 126.97, 124.36, 122.40, 119.69, 119.05, 116.01, 56.29. ESI-MS: m/z calcd for $C_{20}H_{17}NO_2$ [M+H]⁺ 304.4, found 303.9.

5.1.1.41. (4-Chlorophenyl)(2-((3-ethoxy-2-hydroxybenzylidene)amino)phenyl)methanone (**41**). ¹H NMR (400 MHz, DMSO) δ 8.89 (s, 1H), 7.72 (t, J = 11.3 Hz, 3H), 7.59 (d, J = 8.6 Hz, 3H), 7.48 (m, 2H), 7.14 (s, 1H), 7.05 (s, 1H), 6.83 (s, 1H), 3.99 (q, 2H), 1.29 (t, 3H). ¹³C NMR (101 MHz, DMSO) δ 196.34, 167.91, 150.26, 147.04, 145.82, 138.43, 137.79, 133.62, 131.15, 130.86, 130.26, 128.68, 127.41, 125.23, 120.04, 119.78, 119.07, 117.63, 65.84, 15.61. ESI-MS: m/z calcd for $C_{22}H_{18}ClNO_3$ [M+H]⁺ 380.8, found 380.7.

5.1.1.42. 3-((3-Ethoxy-2-hydroxybenzylidene)amino)benzoic acid (**42**). ¹H NMR (400 MHz, DMSO) δ 13.18 (s, 1H), 13.03 (s, 1H), 9.04 (s, 1H), 7.93 (s, 1H), 7.89 (d, J = 7.6 Hz, 1H), 7.68 (d, J = 8.2 Hz, 1H), 7.60 (t, J = 7.8 Hz, 1H), 7.29 (d, J = 7.8 Hz, 1H), 7.15 (d, J = 8.0 Hz, 1H), 6.91 (t, J = 7.9 Hz, 1H), 4.09 (q, J = 6.9 Hz, 2H), 1.36 (t, J = 6.9 Hz, 3H). ¹³C NMR (101 MHz, CDCl₃) δ 170.51(s), 164.05, 151.94, 148.95, 147.93, 130.88, 129.84, 128.64, 127.55, 124.35, 122.02, 119.39, 118.93, 117.14, 64.98, 15.07. ESI-MS: m/z calcd for $C_{16}H_{15}NO_4$ [M+H]⁺ 286.3, found 286.7.

5.1.1.43. 2-((3-Ethoxy-2-hydroxybenzylidene)amino)-6-methylbenzoic acid (**43**). ¹H NMR (400 MHz, DMSO) δ 13.34 (s, 1H), 13.00 (s, 1H), 8.97 (s, 1H), 7.48–7.35 (m, 2H), 7.23 (d, J = 7.2 Hz, 2H), 7.13 (d, J = 7.9 Hz, 1H), 6.90 (t, J = 7.9 Hz, 1H), 4.08 (m, 2H), 2.33 (s, 3H), 1.36 (s, 3H). ¹³C NMR (101 MHz, DMSO) δ 169.89, 164.42, 151.09, 147.50, 144.62, 135.03, 132.14, 130.15, 128.87, 124.71, 119.61, 119.03, 117.42, 115.61, 64.46, 19.29, 15.19. HRMS (ESI): m/z calcd for $C_{17}H_{17}NO_4$ [M+H]⁺ 300.1230, found 300.1233.

5.1.1.44. 2-Ethoxy-6-(((4-methoxyphenyl)imino)methyl)phenol (**44**). ¹H NMR (400 MHz, DMSO) δ 13.53 (s, 1H), 8.94 (s, 1H), 7.43 (d, J = 8.8 Hz, 2H), 7.20 (d, J = 7.7 Hz, 1H), 7.09 (d, J = 7.9 Hz, 1H), 7.03 (d, J = 8.9 Hz, 2H), 6.88 (t, J = 7.9 Hz, 1H), 4.07 (d, J = 7.0 Hz, 2H), 3.80 (s, 3H), 1.35 (s, 3H). ¹³C NMR (101 MHz, DMSO) δ 161.75, 158.97, 151.19, 147.42, 140.88, 124.35, 122.98, 119.82, 118.85, 117.04, 115.07, 64.51, 55.77, 15.20. ESI-MS: m/z calcd for $C_{16}H_{17}NO_3$ [M+H]⁺ 272.3, found 272.1.

5.1.1.45. 2-(((1,1'-Biphenyl)-4-ylimino)methyl)-6-ethoxyphenol (**45**). ¹H NMR (400 MHz, DMSO) δ 11.94 (s, 1H), 8.90 (s, 1H), 7.74 (d, J = 8.6 Hz, 2H), 7.70 (s, 1H), 7.60 (d, J = 8.6 Hz, 3H), 7.49 (m, 2H), 7.14 (d, J = 6.5 Hz, 1H), 7.08 (s, 1H), 6.84 (s, 1H), 4.01 (s, 2H), 1.32 (s, 3H). ¹³C NMR (101 MHz, DMSO) δ 163.91, 151.36, 147.50, 147.36, 139.77, 139.20, 129.41, 128.12, 127.98, 126.98, 124.56, 122.40, 119.79, 119.04, 117.49, 64.56, 15.21. HRMS (ESI): m/z calcd for $C_{21}H_{19}NO_2$ [M+H]⁺ 318.1489, found 318.1490.

5.1.1.46. (2-((3-Ethoxy-2-hydroxybenzylidene)amino)phenyl)(phenyl)methanone (**46**). ¹H NMR (400 MHz, DMSO) δ 12.03 (s, 1H), 8.91 (s, 1H), 7.74 (d, J = 7.3 Hz, 2H), 7.66 (s, 2H), 7.61 (s, 1H), 7.53 (s, 2H), 7.48 (s, 2H), 7.14 (d, J = 7.8 Hz, 1H), 7.06 (d, J = 7.9 Hz, 1H), 6.83 (s, 1H), 4.00 (s, 2H), 1.29 (s, 3H). ¹³C NMR (101 MHz, DMSO) δ 196.94, 164.93, 150.76, 147.24, 146.62, 137.15, 134.79, 134.12,

131.99, 129.96, 129.26, 128.66, 127.11, 124.56, 119.64, 119.38, 119.05, 117.62, 64.44, 15.10. HRMS (ESI): m/z calcd for $C_{22}H_{19}NO_3$ [M+H]⁺ 346.1438, found 346.1440.

5.1.1.47. 3-((2,3-Dihydroxybenzylidene)amino)benzoic acid (**47**). ¹H NMR (400 MHz, DMSO) δ 13.25–13.07 (s, 1H), 12.92 (s, 1H), 9.25 (s, 1H), 9.00 (s, 1H), 7.97–7.85 (m, 2H), 7.67 (d, J = 8.0 Hz, 1H), 7.60 (t, J = 7.8 Hz, 1H), 7.16 (d, J = 7.6 Hz, 1H), 6.97 (d, J = 7.7 Hz, 1H), 6.81 (t, J = 7.7 Hz, 1H). ¹³C NMR (101 MHz, DMSO) δ 167.34, 165.31, 149.66, 148.75, 146.03, 132.59, 130.23, 127.92, 126.37, 123.34, 122.15, 119.83, 119.65, 119.30. HRMS (ESI): m/z calcd for $C_{14}H_{11}NO_4$ [M+H]⁺ 258.0761, found 258.0761.

5.1.1.48. 2-((2,3-Dihydroxybenzylidene)amino)-6-methylbenzoic acid (**48**). ¹H NMR (400 MHz, DMSO) δ 13.29 (s, 1H), 12.78 (s, 1H), 9.22 (s, 1H), 8.91 (s, 1H), 7.42 (s, 1H), 7.36 (s, 1H), 7.22 (s, 1H), 7.11 (s, 1H), 6.97 (s, 1H), 6.80 (s, 1H), 2.33 (s, 3H). ¹³C NMR (101 MHz, DMSO) δ 169.94, 164.80, 149.46, 146.05, 144.92, 135.00, 131.96, 130.21, 128.75, 123.52, 119.78, 119.76, 119.31, 115.83, 19.33. ESI-MS: m/z calcd for $C_{15}H_{13}NO_4$ [M+H]⁺ 272.3, found 272.7.

5.1.1.49. 3-(((4-Methoxyphenyl)imino)methyl)benzene-1,2-diol (**49**). ¹H NMR (400 MHz, DMSO) δ 13.41 (s, 1H), 9.14 (s, 1H), 8.90 (s, 1H), 7.43 (d, J = 8.8 Hz, 2H), 7.05 (dd, J = 13.5, 8.3 Hz, 3H), 6.92 (d, J = 7.6 Hz, 1H), 6.78 (t, J = 7.8 Hz, 1H), 3.80 (s, 3H). ¹³C NMR (101 MHz, CDCl₃) δ 160.3, 159.2, 149.9, 145.4, 140.6, 122.9, 122.4, 119.0, 118.7, 117.4, 114.9, 55.8. ESI-MS: m/z calcd for $C_{14}H_{13}NO_3$ [M+H]⁺ 244.2, found 244.4.

5.1.1.50. (4-Chlorophenyl)(2-((2-hydroxy-3-methoxybenzyl)amino)phenyl)methanone (**50**). ¹H NMR (400 MHz, DMSO) δ 8.68 (s, 1H), 7.37 (m, 4H), 7.00 (m, 2H), 6.81 (d, J = 7.9 Hz, 1H), 6.62 (t, J = 7.8 Hz, 1H), 6.53 (m, 2H), 6.46 (d, J = 8.1 Hz, 1H), 6.16 (d, J = 4.3 Hz, 1H), 4.21 (s, 2H), 3.79 (s, 3H). ¹³C NMR (101 MHz, DMSO) δ 147.59, 146.31, 144.19, 143.36, 131.55, 128.68, 128.55, 128.17, 128.14, 126.49, 120.21, 118.87, 115.78, 110.91, 110.58, 56.17, 41.52. HRMS (ESI): m/z calcd for $C_{21}H_{18}ClNO_3$ [M+H]⁺ 368.1048, found 368.1050.

5.2. Cellular assays

5.2.1. Secreted embryonic alkaline phosphatase (SEAP) and specificity experiments

HEK-TLR2 cells were cultured with a medium made of DMEM as well as 10% PBS and 1% penicillin/streptomycin. On the first day, 200 μ l cells culture medium (4×10^4 cells per well) was added to the 96-well plates for 24 h at 37 °C incubator. Then, the medium was changed to DMEM with indicated concentration of compounds as well as Pam₃CSK₄ (final conc. 10 ng/ml) with totally 200 μ l medium, and incubated it at 37 °C for another 24 h. Finally, 50 μ l Quanti-Blue (invivoGen) and 50 μ l cellular supernatant was added into a new 96-well plate. After 15–30 min, you can observe the emergence of metachromatism, and then test the optical density at 620 nm. As for specificity experiment, replace the positive with respectively specific TLR agonist (10 ng/ml Pam₃CSK₄ for TLR1/2, 10 ng/ml Pam₂CSK₄ for TLR2/6, 10 μ g/ml Poly I:C for TLR3). HEK-Blue hTLR2 and HEK-Blue hTLR3 cells were employed in the specific assay.

5.2.2. Cell toxicity assay

HEK-TLR2 cells were cultured with a DMEM medium made of 10% FBS and 1% penicillin/streptomycin. On the first day, the culture medium containing the cells (4×10^4 cell per well) was added to the 96-flash plate at a volume of 200 μ l for 24 h. The next day, the medium was changed to DMEM only and added positive

control Pam₃CSK₄ (final conc. 10 ng/ml), as well as indicated concentration compounds to 200 μ l totally, then incubated for 24 h. On the third day, 20 μ l of 5 mg/ml MTT (in PBS) solution was added to each well of the above 96-well plate, and then placed in 37 °C incubator for 3 h, gently suck the medium out and buckled the 96 wells plate overnight. Next, 100 μ l of DMSO was added to each well of the 96-well plate, shaken for 1 h and measured at an absorbance of 490 nm through a plate reader.

5.2.3. Nitric oxide assay

Raw 264.7 cells were cultured with a RPMI 1640 medium made of 10% PBS, 1% penicillin/streptomycin. On day one, the culture medium containing cells (8×10^4 cell per well) was added to the 96-well plates for 24 h at 37 °C incubator. Then replaced the media, added compound and RPMI 1640 only to 200 μ l totally, and it was incubated for 24 h also. 100 μ l supernatant and 10 μ l DAN (2,3-diaminonaphthalene, 0.05 mg/ml DAN dilute in 0.62 M aqueous HCl) were drawn to flat black 96-well microfluor plates for 15 min' incubation in the dark. 5 μ l NaOH solvent (3 mol/L) was added and read on Infinite M100 Pro (Tecan) reader with excitation at 365 nm and emission at 410 nm in 10 min.

5.2.4. Cytokine ELISA assays

PBMC, peripheral blood mononuclear cells, were seeded in twelve-well plates at a density of 2.5×10^5 cells per well with 0.5 mL of medium [RPMI 1640 medium supplemented with 10% FBS, and 1% penicillin/streptomycin]. The cells were treated with indicated concentrations of SMU-A0B13 and 10 ng/ml Pam₃CSK₄ (Invivogen) as positive control and incubated for 24 h at 37 °C in a 5% CO₂ humidified incubator. The cell culture supernatants were collected and frozen at –80 °C until measurement. The level of cytokine TNF- α was determined using recombinant human-cytokine standards, cytokine-specific capture antibodies and detection antibodies according to the commercially available ELISA kit (BD Biosciences) with each sample for triplicate.

5.2.5. Immunoblot analysis

Entire proteins from antagonist-treated cells were extracted with PIPA solution involving 1% PMSF (both from Life Sciences). These proteins were separated using the SDS-PAGE (Life Sciences) and transferred onto PVDF membranes (Merck Millipore). Membranes were blocked with 5% (w/v) skim milk (Becton, Dickinson and Company) in TBST and incubated with TLR2 or GAPDH primary antibody overnight at 4 °C on the shaker. After washed for five times with TBST, membranes were incubated with their respective secondary antibody for 1 h in RT on the shaker. Detection was performed with ECL Chemiluminescent Substrate Reagent Kits (Life Sciences) and the FluorChem R Multifunctional Imaging Analysis System (ProteinSimple). During this operation, the following primary and secondary antibodies were employed: rat-GAPDH (1:2000, Life Sciences), rat-TLR2 (1:250, Boster), goat-anti-rat-GAPDH/TLR2-HRP (1:2500, Boster).

5.2.6. Molecular docking modeling

All molecular docking calculations were performed with the help of Autodock vina 1.1.2 based on the crystal structure of the TLR2 TIR domain (PDB: 1FYW). All rotatable bonds of compounds were set rotatable and the residues of the BB loop pocket (Y647, C673, D678, F679, I680, K683, D687, N688, D691 and S692) were chose as Flexible Residues. The box was centered on (14.249, 95.837, 13.802) and the number of points in each dimension is 50 which spaces 0.375 Å.

Acknowledgments

This work was supported, in part, by the scientific research project of high level talents (No. C1033269) in Southern Medical University of China, Youth Pearl River Scholar Program of Guangdong Province (No. C1034007), Science and Technology Planning Project of Guangdong Province, China (No. 2014750) and Innovation and Entrepreneurship of college students in Guangdong (No. C1033579), as well as National Natural Science Foundation of China (No. 81773558).

A. Supplementary data

Supplementary data associated with this article can be found, in the online version, at <https://doi.org/10.1016/j.bmc.2018.03.001>.

References

1. Kanzler H, Barrat FJ, Hessel EM, Coffman RL. *Nat Med*. 2007;13:552–559.
2. Iwasaki A, Medzhitov R. *Nat Immunol*. 2004;5:987–995.
3. Takeda K, Akira S. *Int Immunol*. 2005;17:1–14.
4. Akira S, Takeda K. *Nat Rev Immunol*. 2004;4:499–511.
5. Akira S, Takeda K, Kaisho T. *Nat Immunol*. 2001;2:675–680.
6. Hamerman JA, Pottle J, Ni M, He Y, Zhang ZY, Buckner JH. *Immunol Rev*. 2016;269:212–227.
7. Liu PT, Stenger S, Li H, et al. *Science*. 2006;311:1770–1773.
8. Zarembek KA, Godowski PJ. *J Immunol*. 2002;168:554–561.
9. Castoldi A, Braga TT, Correa-Costa M, et al. *PLoS ONE*. 2012;7:e37584.
10. Yang HZ, Cui B, Liu HZ, et al. *PLoS ONE*. 2009;4:e6520.
11. Horton CG, Farris AD. *Curr Allergy Asthm R*. 2012;12:1–7.
12. Malley R, Henneke P, Morse SC, et al. *Proc Natl Acad Sci U S A*. 2003;100:1966–1971.
13. Shin HS, Xu F, Bagchi A, et al. *J Immunol*. 2011;186:1119–1130.
14. Kawai T, Akira S. *Nat Immunol*. 2010;11:373–384.
15. Wang J, Hu Y, Deng WW, Sun B. *Microbes Infect*. 2009;11:321–327.
16. Oliveira-Nascimento L, Massari P, Wetzler LM. *Front Immunol*. 2012;3:79.
17. Shizuo A, Satoshi U, Osamu T. *Cell*. 2006;783–801.
18. Reilly M, Miller RM, Thomson MH, et al. *Clin Pharmacol Ther*. 2013;94:593–600.
19. Zhang Y, Luo F, Cai Y, et al. *J Immunol*. 2011;186:1963–1969.
20. Murata M. *Cancer Sci*. 2008;99:1435–1440.
21. Cheng K, Gao M, Godfroy JI, Brown PN, Kastelowitz N, Yin H. *Sci Adv*. 2015; e1400139.
22. Cheng K, Wang X, Zhang S, Yin H. *Angew Chem Int Ed Engl*. 2012;51:12246–12249.
23. Meng G, Rutz M, Schiemann M, et al. *J Clin Invest*. 2004;113:1473–1481.
24. Murgueitio MS, Henneke P, Glossmann H, Santos-Sierra S, Wolber G. *ChemMedChem*. 2014;9:813–822.
25. Koymans KJ, Feitsma LJ, Brondijk TH, et al. *Proc Natl Acad Sci USA*. 2015;112:11018–11023.
26. Mauldin IS, Wang E, Deacon DH, Olson WC, Bao Y, Slingluff CJ. *Int J Cancer*. 2015;137:1386–1396.
27. Zhou S, Cerny AM, Bowen G, et al. *Antiviral Res*. 2010;87:295–306.
28. Mistry P, Laird MH, Schwarz RS, et al. *Proc Natl Acad Sci USA*. 2015;112:5455–5460.
29. Malakyan M, Babayan N, Grigoryan R, et al. *F1000Res*. 2016;5:1921.